Physics – Uspekhi **52** (1) 165 – 178 (2009)

INSTRUMENTS AND METHODS OF INVESTIGATION PACS numbers: 79.20.Rf, **81.07. – b**, **81.16. – c**

Physical mechanisms underlying the selective removal of atoms

B A Gurovich, K E Prikhod'ko

DOI: 10.3367/UFNe.0179.200902d.0179

Contents

Abstract. This paper reviews the current understanding of the selective removal of atoms (SRA), a technique that uses ion irradiation to controllably change the chemical composition and properties of polyatomic materials. The main effects involved and the possible mechanisms that govern the process are discussed. It is shown that SRA holds great promise for manufacturing functional nanoelements.

1. Introduction

The experiments in Refs [1 – 4] introduced irradiation by accelerated particles as a tool for selectively removing atoms from di- or polyatomic chemical compounds. Such removals, along with radically changing the chemical composition and chemical properties of the compound, also produce no less radical changes in physical processes, giving rise to nonmetal–metal, dielectric–semiconductor, and nonmagnetic–magnetic transitions, markedly affecting the optical properties, changing the volume of the material, and so on. In another aspect of this technique, the composition and properties of the material can be manipulated on a very small spatial scale (currently already ~ 15 nm), potentially leading to arbitrary-geometry composite structures of wide application.

There are, however, some questions concerning the nature of the observed phenomenon, with the role of diffusion processes perhaps topping the list, that cannot be answered based on the experimental data in Refs [1 – 4]; the undoubtedly appealing prospects of directly forming functional elements has clearly necessitated the experimental study of the underlying mechanisms and potential applications of SRA.

It is with this in mind that we have conducted an experimental study of SRA mechanisms possibly involved in the spatially localized modification of the composition and properties of various chemical compounds. The present paper summarizes the results of this study. It discusses the role of diffusion processes in SRA and deepens insight into the nature of SRA by estimating, among others things, how much the material property transformations can possibly be localized; how profoundly the composition and properties of the material can be changed; and how close together the elements of the prospective composite structures can be.

B A Gurovich, K E Prikhodko Russian Research Center
'Kurchatov Institute,'
pl. Kurchatova 1, 123182 Moscow, Russian Federation
Tel. (7-499) 196 94 14, (7-499) 196 92 15
Fax (7-499) 196 17 01
E-mail: ba_gurovich@irtm.kiae.ru, kirill@irmrnt.kiae.ru

Received 16 July 2008, revised 7 October 2008
Uspekhi Fizicheskikh Nauk **178** (2) 179 – 195 (2009)
DOI: 10.3367/UFNr.0179.200902d.0179
Translated by E G Strel'chenko; edited by A M Semikhatov

2. Experimental results

We used the following experimental techniques (see Refs [1 – 5] for more details) to study the effects accompanying SRA in irradiated materials:

— the method of measuring the electric resistance of thin films in planar geometry;

— X-ray photoelectron spectroscopy (XPS), occasionally with layer-by-layer etching (the technique was used to study radiation-induced chemical composition changes in thin films);

— electron microscopy techniques, including dark and bright field transmission microscopy of thin films and the analysis of transmission and reflection electron diffraction patterns (to monitor how the phase composition and structure of a thin film evolve in the course of irradiation, to determine the grain size and lattice parameters, and to identify the material of the film before and after irradiation);

— thin film profilometry (to measure film thicknesses before and after irradiation);

— vibrational magnetometry (to obtain thin film magnetization curves before and after irradiation and to measure key magnetic characteristics such as the saturation magnetization, residual magnetization, and coercitivity);

— scanning atomic force microscopy (AFM) and magnetic force microscopy (MFM) (to study mask topography and the effect of radiation on the film surface relief, as well as to visualize the magnetic fields of nanoscale particles produced by SRA radiation).

Based on the experimental results on the effect of ion radiation on the chemical composition and properties of a substance, the following key points can be made concerning the SRA process:

1. Although we also used electron and helium atom irradiation to implement and observe the selective removal of atoms, most of our experimental data were obtained with proton irradiation [1–4]. One indication of the reduction of elements from a chemical compound is that the electric resistance of a film changes to a pure-element value as the film is irradiated. Figure 1 shows the typical electric resistance versus radiation dose curves for films of the oxides CuO, GeO_2, BiO_2, Fe_2O_3, WO_3, NiO_2, Co_3O_4, and Ta_2O_5 irradiated by protons of different energies. It is seen that at a certain dose level, films of all these materials reveal a marked decrease in the electric resistance, indicating the removal of oxygen atoms from the compounds. According to Ref. [6], films of reduced metals have the electric resistivity similar to that of films of sputtered pure metals of the same thickness. In earlier studies (see, e.g., Ref. [1]) it was shown that for long enough exposures, XPS spectra show virtually no lines of the elements being removed, implying that complete reduction occurs. It was also found that in films of reduced metals, the temperature dependence of the electric resistance is typically of the metallic type (see, e.g., Ref. [1]).

For some of the materials listed above (for example, the oxide BiO_2) we showed in Ref. [7] that they can be reduced by irradiation with 200 keV electrons. In the same reference, we used transmission electron microscopy to demonstrate successive composition changes occurring in thin films, during which irradiation by electrons in the electron microscope column gives rise to intermediate, lower oxygen content oxides, up to the complete reduction of the metal as confirmed by the diffraction pattern.

The analysis of electron diffraction patterns has shown that irradiating thin films of Fe_2O_3 and WO_3 by ~ 1 keV helium ions also causes the reduction of iron and tungsten, as indicated by the appearance of pure-metal diffraction lines.

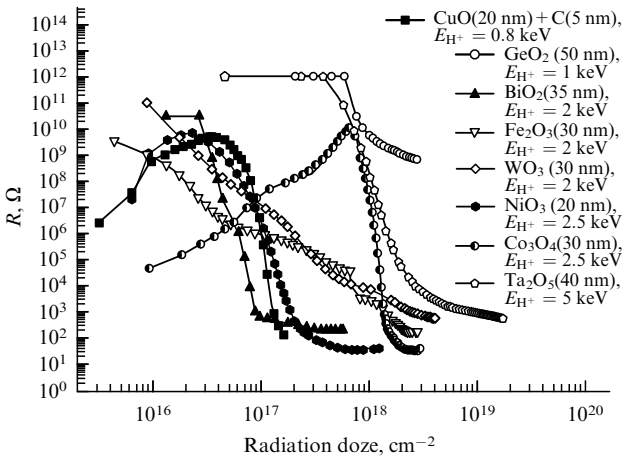

Figure 1. Planar electric resistance versus dose for films of metal oxides (CuO, GeO_2, BiO_2, Fe_2O_3, WO_3, NiO_2, Co_3O_4, Ta_2O_5) irradiated by protons of various energies.

That metals can be reduced by irradiating oxides with charged particles like protons, electrons, and helium ions implies that SRA has no relation to the interaction of accelerated particles with the material being irradiated but is of a radiative nature, i.e., is caused by atomic displacements due to irradiation by accelerated particles.

This was confirmed by the discovery that the irradiation-induced reduction of cobalt oxide is a threshold process. It was shown, specifically, that cobalt oxide films are not reduced when exposed over a long period of time to plasma containing some amount of active atomic hydrogen along with low-energy protons. In these experiments a (zero-bias) sample was irradiated with ~ 50 eV protons from a high-frequency hydrogen plasma. Despite the high radiation doses used (which were conservatively taken to be three times what suffices to completely reduce the same oxide film at proton energies of 600 eV at the same plasma parameters), no magnetic properties were detected in the samples, conclusively indicating that the proton energy 50 eV is insufficient for the SRA process to operate in cobalt oxide.

By applying a negative bias voltage to the sample, a flux of protons of appropriate energy was obtained, which was used to irradiate cobalt oxide. It was established that using protons of the energy 300 eV or higher did reduce cobalt, as could be inferred from the appearance of magnetic properties in the irradiated regions of the sample. Because the experiments did not allow accelerating ions to intermediate energies, it was impossible to accurately determine the threshold energy for displacing oxygen atoms in the cobalt oxide. However, the results obtained in these experiments indicate beyond doubt the threshold nature of the SRA process.

2. The selective removal of atoms from oxides, nitrides, and some other types of chemical compounds leads to the virtually complete reduction of the corresponding elements. Evidence for this includes XPS spectra [1, 2], electron diffraction data [1, 3], data on electric [1, 6] and magnetic [1] properties, and volume change measurements on irradiated films [5]. The discussion below lists some typical experimental results on this effect.

In Fig. 2, which shows a typical change in the XPS spectrum following the exposure of germanium oxide (GeO_2) to 2 keV protons, the disappearance of the oxygen peak suggests a virtually complete reduction of germanium from the oxide as a result of proton irradiation.

Figure 3 presents the magnetization behavior of a film of cobalt reduced from the oxide by 3 keV proton irradiation.

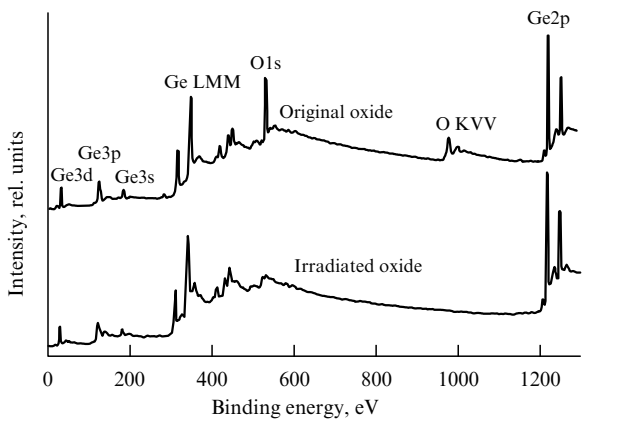

Figure 2. XPS spectra of a germanium oxide film before and after proton irradiation.

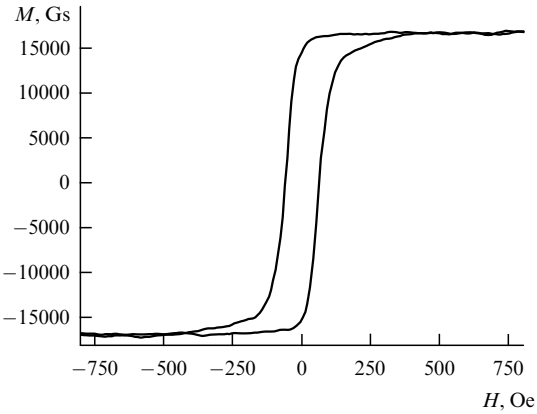

Figure 3. Magnetization curve of a film of cobalt reduced from oxide by exposure to 3 keV proton radiation.

The original oxide and the film of reduced cobalt had the respective thicknesses (60 ± 1) nm and (24 ± 1) nm and, based on the data presented in the figure, the saturation magnetization was (17.0 ± 0.9) kGs. The last value agrees well with tabulated magnetization data on pure cobalt, thus implying the complete through-thickness reduction of the film.

Increasing ion energy within our investigated range ($\sim 0.3-5$ keV) increases the depth of the reduced layer. Referring to Fig. 4a, increasing the proton energy reduces the ultimate resistance of the irradiated 40 nm cobalt oxide film, indicating that the reduction thickness of cobalt oxide increases with increasing the proton energy. At the same time, for a thinner (20 nm) oxide film, the ultimate resistance is practically independent of the proton energy (Fig. 4b), implying that in this case, the oxide film is reduced completely for all proton energies studied. Such a method of irradiating films of a given thickness by protons of various energies can provide an estimate of the proton beam energy needed to completely reduce the film throughout its thickness. Figure 4c shows SRIM [8] calculations of the hydrogen ion distribution profile over the thickness of a cobalt oxide sample for the proton energies 0.8, 1.2, and 1.6 keV. It is seen that the reduction depths derived from the dose dependences in Figs 4a, b approximately correspond to the projective range of protons of the corresponding energies.

Another way to determine the complete reduction depth is by measuring the shrinkage, a decrease in the thickness of the layer due to SRA. As shown earlier [5], SRA involves a considerable thinning of the irradiated layer due to a marked decrease in the number of its constituent atoms. The experimental measure of volume decrease under the condition of film continuity is the shrinkage S, the thickness ratio of the irradiated to the original film. Ultimately, after completely removing light atoms (for example, oxygen), the shrinkage can be greater than ~ 0.5. Table 1 lists measured shrinkages for a number of investigated compounds (Co_3O_4, Fe_2O_3, NiO, BiO_2, CuO, WO_3, MoO_3, and PtO) whose films of 40 nm in thickness were irradiated by 2 keV protons [5]. The good agreement between the experimental and calculated shrinkage values suggests that the oxides listed in the table are reduced completely throughout the film thickness.

One possible way of determining the reduction depth of a material subject to a fixed-energy proton radiation is by analyzing how the thickness of an irradiated film depends on the original thickness of the film. Figure 5 plots such a dependence for the reduction of cobalt from cobalt oxide

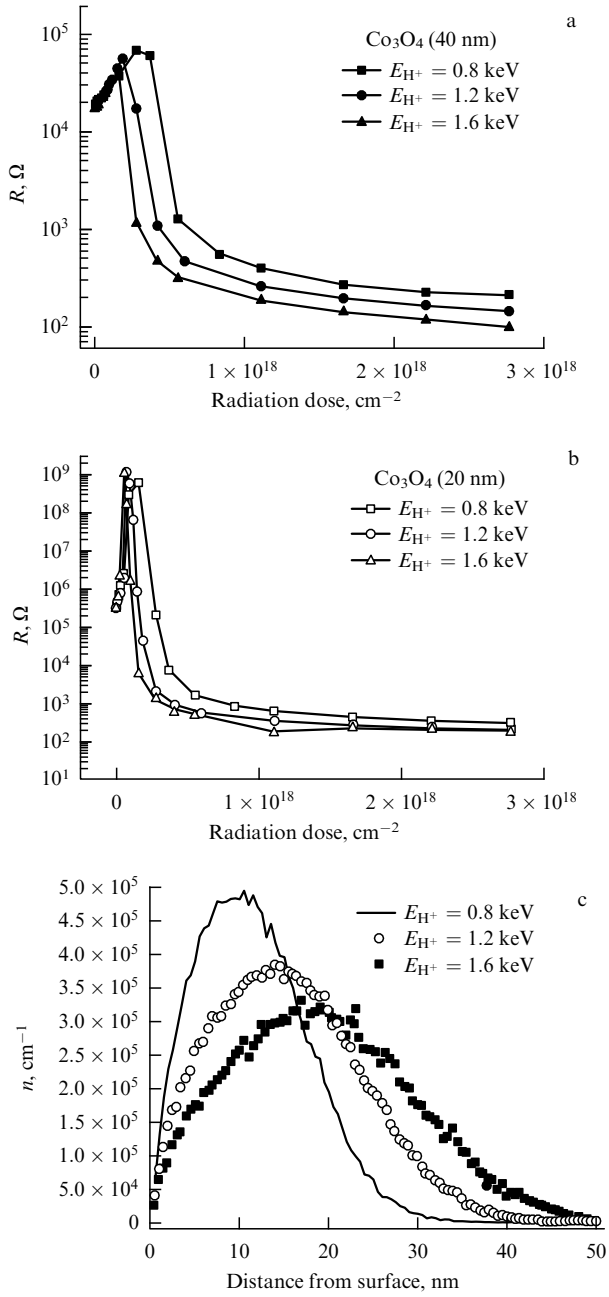

Figure 4. Electric resistance versus dose for Co_3O_4 films of the thickness 40 nm (a) and 20 nm (b) irradiated by protons of the energy 0.8, 1.2, and 1.6 keV. (c) SRIM results for hydrogen ion concentration profiles along the depth of cobalt oxide for protons of the energy 0.8, 1.2, and 1.6 keV [13].

Co_3O_4 at the proton energy 3 keV. It is seen that at low original thicknesses, the thickness of the reduced film exhibits a linear dependence. In this region, the film is completely reduced throughout the entire thickness of the original oxide film, and the slope in the linear region corresponds to the measured value of shrinkage. As the thickness of the oxide film increases, the dependence is seen to depart from linear, indicating that the oxide fails to be reduced throughout its entire thickness. We thus see that the dependence shown in Fig. 5 provides both the experimental value of shrinkage and an estimate for the maximum depth of film modification for a fixed proton energy.

As the shrinkage experiments of Fig. 5 suggest, the maximum original film thickness of the cobalt oxide fully

Table 1. Calculated versus experimental values of proton-irradiation-assisted shrinkage of 40 nm thick oxide films [11].

Material	S_{cal}	S_{exp}
Co_3O_4	0.36	0.38 ± 0.03
Fe_2O_3	0.47	0.49 ± 0.03
NiO	0.62	0.60 ± 0.03
BiO_2	0.84	0.84 ± 0.03
CuO	0.59	0.61 ± 0.03
WO_3	0.34	0.37 ± 0.05
MoO_3	0.31	0.37 ± 0.05
PtO	0.61	0.62 ± 0.03

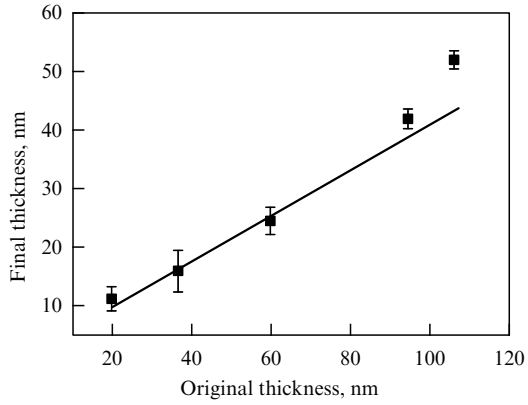

Figure 5. Thickness of a reduced cobalt film versus the original thickness of a Co_3O_4 film for the proton energy 3 keV.

reduced to metal by exposure to ~ 3 keV protons is $\sim 90-100$ nm, which agrees quite well with the SRIM projected range calculations [8].

3. The experiments we conducted showed that for most of the chemical compounds studied, SRA proton irradiation works over the entire accessible range of accelerating voltages, $\sim 300-5000$ eV. These experiments typically used some of the techniques mentioned above (XPS, electron diffraction, electric resistance, magnetic properties, shrinkage measurements, etc.) to detect the occurrence of the SRA process. The available experimental results of this kind, which are reviewed in fine detail in Refs [1–6, 9, 10], indicate that a similar process is also likely to occur with higher-energy accelerated protons. However, the energies we used are quite sufficient for many promising applications, such as functional nanoelements for various uses (see Ref. [11]).

Among the large number of chemical compounds that we studied for the possibility of SRA, those studied most systematically were the oxides of Pt, Pd, Ag, Co, Cu, Re, Bi, W, Pb, Sn, Ge, Mo, Ni, Fe, Ga, Ta, Ti, Nb, and V. As noted above, accelerated protons were used for irradiation in most cases. The reasons for this were several and included: the projected range of protons is larger than that of other ions of the same energy; for many of the materials treated, it is known that hydrogen can leave the material very soon after the irradiation is over; and the backscattering effect is small (which is important for designing high-density nanoelements).

In a number of cases, SRA patterned structures that were held in air at room temperature for about 5 years, with no protective layers on them, and showed no change in their service performance. Examples are patterned magnetic structures obtained by the irradiation of cobalt oxide. That these structures retained their properties for that long could be seen from the measured values of their magnetic characteristics. Heating the samples in a vacuum to temperatures $\sim 250\,^{\circ}C$ for a period of one hour also left their properties unchanged. In some cases, however, to avoid property degradation, the obtained structures had to be covered by protective layers or protected by other means, similarly to how microelectronic devices are protected.

Two important points about the selective removal of atoms were noted in Refs [1–4]:

(1) When using SRA, radical composition changes in a chemical compound (to the point of completely removing one atomic species) can be achieved not only by direct exposure but also by irradiation through intermediate layers of other materials, monatomic or of a more complex nature. Importantly, the intermediate layers can retain their composition during the treatment (Fig. 6).

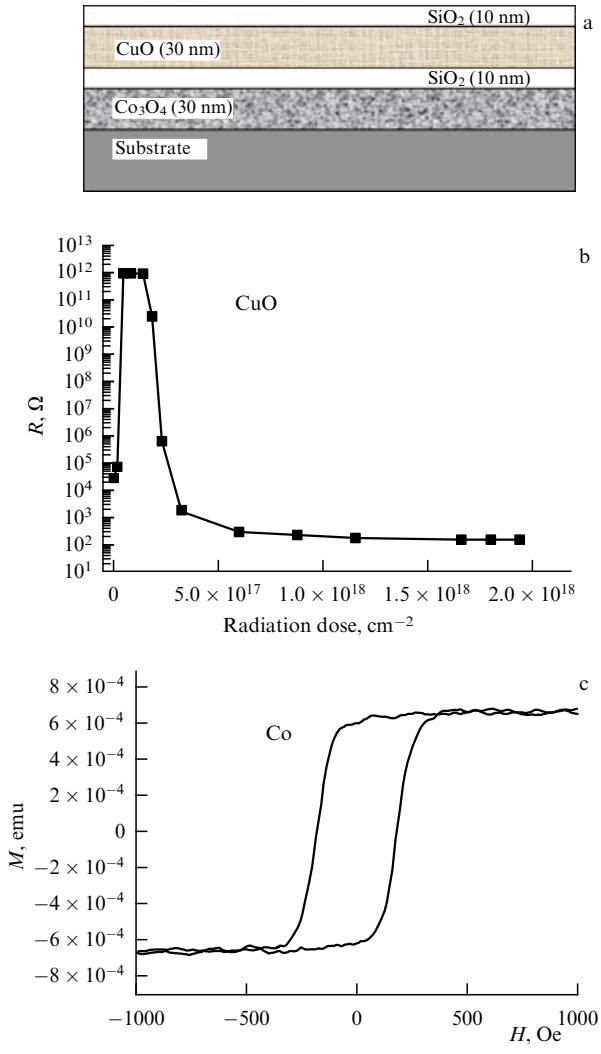

Figure 6. (a) Schematic of a multilayer sample: a substrate of monocrystalline silicon supports layers of Co_3O_4 (30 nm), SiO_2 (10 nm), CuO (30 nm), and SiO_2 (10 nm). (b) Resistance of a copper oxide film versus radiation dose for 1 keV proton radiation. (c) Magnetization curve after irradiation.

(2) When using SRA, radical composition changes in a chemical compound (in particular, when irradiated through intermediate layers with the thickness ~ 50 nm) occur at depths corresponding to the projected range of the accelerated particles used (see Fig. 6).

The results presented in Fig. 6 demonstrate how the SRA process works in a multilayered 80 mm thick sample. As seen from Fig. 6b, proton irradiation reduces copper and cobalt in each of the working layers despite the presence of a neighboring layer and of two intermediate silicon dioxide layers. This indicates that SRA holds promise for producing transformations in all the layers of multilayered structures simultaneously: a solution, in principle, to the compatibility problem for elements in the different layers of a nanoscale structure under design.

The experimental results presented above indicate without a doubt that SRA has no relation to the mechanical (i.e., collisional) sputtering of atoms, i.e., their escaping from the surface of the irradiated material due to primary interaction events between the accelerated particles and the material's atoms located in near-surface layers a few angstroms thick.

Another category of evidence for the complex nature of SRA comes from our observation that the rate of SRA-produced change in the composition of chemical compounds is strongly temperature dependent (see the discussion below).

It therefore seems appropriate to turn again to the underlying physical mechanisms of SRA.

3. The nature of the SRA process

In Ref. [1], the selective removal of atoms of a given species from a proton-irradiated material is considered to be mainly due to the displacement selectivity of these atoms in the process of irradiation. In this context, the term selectivity means that atoms of one species in a di- or polyatomic material have a higher displacement rate than atoms of the other (or others). The displacement selectivity reaches its limit value when the maximum energy transfer $T_{\max}$ becomes larger than the threshold displacement energy E_{d} for atoms of one species and smaller than that for another. The radiation-assisted selective removal of atoms of the first species is realized in full measure, which under certain conditions can lead to their complete removal from the irradiated volume.

The maximum energy transfer from an incident ion of mass m and energy E to a target atom of mass M is given by

$$T_{\max} = 4E\,\frac{mM}{(m+M)^2}\,. \qquad (1)$$

Equation (1) clearly shows that the requirement for atoms of one of the species to undergo no displacement at all imposes severe limitations on the energy of the incident particles.

For example, for protons, the lightest ions of all, the low upper bound on the energy imposes a restriction on the thickness of the material layer being treated (Table 2). This is not likely to be very important when using SRA to create nanosize structures because these are typically no more than ~ 10 thick. At the same time, to use the major advantage of SRA — the ability (shared by few or no other techniques) to transform material properties in several layers at once and thereby to establish the self-compatibility of structural elements ~ 1 nm in size [2] — it is necessary that the radiation-induced transformations occur at large thicknesses, not less than ~ 100 nm. Increasing the thickness of the layer to be modified requires higher incident energies, which may result in the energy transfer becoming many times the threshold value E_{d} for all the atomic species involved and hence displacement processes occur in all the atomic subsystems. The numerous experiments we conducted after the publication of Ref. [1] showed that if the accelerated particles used are light, these energies (see above for more details) also enable atoms of some species (specifically, lighter atoms) to be selectively picked out for removal [2–4]. In this connection, it became clear that the radiation-induced displacement of atoms of only one species in a chemical compound (or alloy) is only a special case of conditions required for selective removal.

Table 2. Maximum energy transfer as a function of the incident proton energy for different target atoms.

E, eV	Chemical element									
	Li	Be	B	N	O	Al	Si	Co	Ta	Bi
500	220	180	155	124	111	69	66	34	11	9
1000	440	360	310	248	222	138	132	66	22	18
3000	1320	1079	930	746	664	376	396	198	66	54

In the general case, two mechanisms of removing atoms from the irradiated zone (i.e., from the zone where radiation defects occur) can be considered:

- atoms are removed purely mechanically as a result of interaction events between accelerated particles and target atoms on the one hand and between target atoms themselves on the other;
- displaced target atoms diffuse toward sinks and then leave the irradiated region (where radiation defects are generated) and occasionally even the target.

Whereas the purely mechanical component of SAR is essentially its athermal part, the diffusional component is temperature dependent. Clearly, the purely mechanical component can only dominate at relatively low (material-specific) irradiation temperatures.

4. The mechanical component of the SRA process

For atoms of a given species to be removed purely mechanically from the irradiation zone (i.e., moved over the entire length of the projected range of the accelerated particles), it is necessary that their successive displacements in the process of irradiation occur in a certain preferred direction. We find the conditions for this to be possible.

The conditions for selectively removed atoms to have directional displacements are most easily satisfied for irradiation by electrons, for which the maximum energy transfer does not much exceed E_{d} (this corresponds to energies of the order of 100–300 keV for electrons). In a polyatomic compound, such conditions may arise simultaneously for several atomic species with similar masses (for much heavier atoms, the maximum energy transfer is less than E_{d} in that case). Atoms are then knocked out in head-on collisions, acquiring a momentum in the direction of the electron (ion) beam. Because a knocked-out atom does not have enough energy for moving in the lattice, it occupies an interstitial position or recombines with the nearest available vacancy, the latter occurring if the atom's distance from the original position is less than or equal to the radius of the spontaneous

recombination sphere. An important point to note is that under the conditions mentioned, each knockout event displaces atoms to one side, in the direction parallel to the beam of accelerated particles. None of the layers lying below is, on the average, depleted of atoms because atoms knocked out from them are replaced by same-species atoms from the layers above. As irradiation and SRA proceed, the depletion boundary moves into the bulk, and at a certain critical depletion level, a phase transformation occurs, which produces either an intermediate composition phase or, if the concentration of knocked-out atoms is already low, a phase of a pure material. This scenario is possible if interstitial atoms (that is, atoms being removed) show practically no diffusion under such conditions. Thus, in the cases where the maximum energy transfer to removed atoms slightly exceeds the threshold displacement energy, the SRA process occurs due to the atoms of a certain species being uniformly displaced along the direction of the beam particles. Each knocked-out atom is displaced over a distance somewhat longer than the radius of the spontaneous recombination sphere, and the phase transformation process starts from the beamward surface of the sample and extends into the bulk as the concentration of the atoms being removed decreases. We observed this effect experimentally by irradiating thin (20 nm) films of bismuth oxide and using an electron microscope at the accelerating voltage 200 kV [7].

For many practical applications, the essential drawbacks inherent in electron irradiation make it a nonoptimal choice for doing SRA. These drawbacks are mainly that the transformation cannot be realized on a macroscopic area within a reasonable time and that the associated backscattering events put an upper limit on the size of elements thus produced. Irradiation with ions shows more promise for SRA as a tool for a targeted modification of material properties.

In the case of ion radiation, the directional removal of atoms is more problematic to achieve than with electrons because ions and targeted atoms are comparable in mass and because the requirement that the momentum of a primary knocked-out atom be preferably along the beam poses severe constraints on the energy of the incident ions. This energy should guarantee a slight excess of the maximum energy transfer $T_{\max}$ over $E_{\rm d}$ (we note that the knock-out rate of atoms is relatively low because the energy transfer from accelerated ions to targeted atoms is unlikely to be sufficient for the latter to be displaced). If $T_{\max} > 2E_{\rm d}$, a knocked-out atom is able to knock out yet another atom, but because the primary and secondary knocked-out atoms have the same energy, the directed displacement condition is not satisfied for the secondary atom. If the above conditions for the directional removal of atoms by ion irradiation are satisfied, purely mechanical SRA becomes possible even at the depth equal to the projected range of the beam ions.

One situation that may arise in the case of directional displacement is when the energy transfer to ions is sufficient for the atoms of either species in the irradiated compound to undergo displacement. If the atoms to be removed are displaced at a much higher rate than the other constituent atoms, then displacement becomes a selective process for atoms of a certain species. The factors leading to the difference in the displacement rates between different species are, among others, the difference in the atomic mass and in the threshold displacement energy.

We consider the situation of different displacement rates in the case where the irradiated material is a diatomic chemical compound. If the sample is exposed to a flux of particles and if the maximum energy transfer exceeds the threshold displacement energy $E_{\rm d}$, the displacement velocity is given by

$$V_{\rm displ} = j\sigma_{\rm d}\,, \tag{2}$$

where $\sigma_{\rm d}$ is the cross section for knocking out atoms with energy transfers between $T_{\max}$ and $E_{\rm d}$, and j is the incident flux density. If the incident particles are light ones with energies of the order of or less than a few keV, their interactions with target atoms are mostly hard-sphere-type collisions, whose cross section is given by [12]

$$\sigma_{\rm d} = \pi r_0^2\left(1 - \frac{E_{\rm d}}{T_{\max}}\right), \tag{3}$$

where

$$r_0 = \frac{a_{\rm B}}{(Z_1^{3/2} + Z_2^{3/2})^{1/2}} \tag{4}$$

is the radius for the full screening of the nuclear Coulomb potential by orbital electrons, Z_1 and Z_2 are the respective atomic numbers of the incident and target atoms, [12], and $a_{\rm B}$ is the Bohr radius. As seen from Eqns (1) and (3), the value of the cross section depends on the incident-to-target mass ratio.

Figure 7 shows cross sections for the displacement of target atoms as functions of the target atomic mass for various incident proton energies. It is seen that the difference in cross sections and hence in the displacement rates between target atoms of widely different masses may be as large as an order of magnitude. For example, for tungsten oxide irradiated with 1 keV protons, assuming that both atoms have the threshold displacement energy 20 eV, oxygen atoms are displaced 50 times as fast as tungsten atoms. Importantly, the displacement cross section data in Fig. 7 are only of qualitative value because the difference in the threshold displacement energies between different atoms in different materials is not considered here. For this reason, the accurate calculation of $\sigma_{\rm d}$ for each compound requires a more accurate knowledge of the value of $E_{\rm d}$. As is known, however, the value of $E_{\rm d}$ lies in the range from ~ 10 eV to ~ 30 eV for a wide

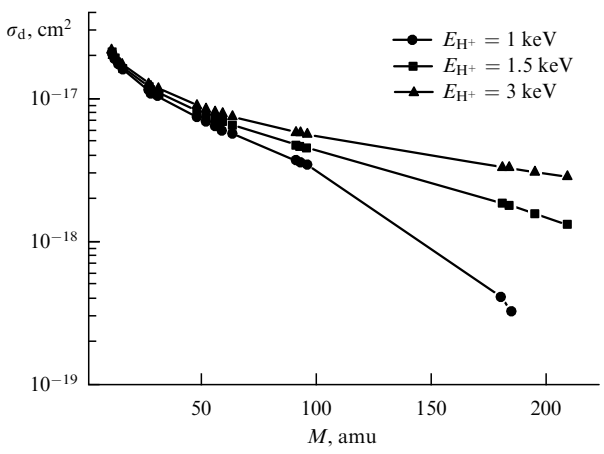

Figure 7. Mass dependence of the displacement cross section for target atoms for different incident proton energies (hard-sphere potential; the threshold displacement energy is taken to be 20 eV for all atoms).

range of materials, which makes 20 eV a good choice for qualitative estimates. The above implies that a marked difference in the displacement rates between atoms of different species in a di- or polyatomic material exposed to proton irradiation can be obtained if proton energies do not exceed a few keV.

Thus, we conclude that if a di- or polyatomic compound is irradiated by accelerated particles with sufficient energy to displace an atom of any constituent species, purely mechanical SRA can be achieved over the entire length of the projected range of the accelerated particles if the thickness of the irradiated region is comparable to this length.

It is important to note that purely mechanical SRA is possible only if there is a large species-to-species difference in the displacement rate in the chemical compound being irradiated.

If T_{max} is much greater than E_d, then atomic displacement events occur with equal probability for all directions or, in other words, their directionality property is completely lost. In this case, given the energy and mass of the primary knocked-out atoms (PKAs), a purely mechanical SRA is only possible in layers one or two atomic spacings thick (similar to physical sputtering). At depths larger than that, without displacements being anywhere directional, all atoms keep their positions unchanged on the average. This is the reason why it is impossible in this case to achieve purely mechanical SRA over the entire length of the projected range.

We next consider how SRA can be realized over the entire length of the projected range in an irradiated material where diffusion processes are importance.

5. The effect of diffusion processes on SRA

As noted above, the displacement of an atom that is to be removed is insufficient for its removal from the irradiated region. One possible mechanism for removing such atoms from the radiation zone is diffusion. Clearly, if the irradiation temperature is sufficient for the targeted atoms to effectively diffuse, the difference in displacement rates between atoms of different species in the irradiated compound is no longer relevant to SRA.

As is known, a necessary condition for atoms to diffuse is that the diffusion mobility and concentration gradient of the atoms be considerable at the relevant scale. It is well known that among several factors determining the diffusion mobility of atoms, the most important one is the diffusion coefficient. The value of the diffusion coefficient is determined by three parameters: the natural hopping frequency of atoms, the probability of finding a nearby site to hop to, and the height of the potential barrier to hopping. The irradiation of a material greatly increases the concentration of defects and thereby greatly affects the diffusion mechanisms at work. It is a well-established and widely observed [13] experimental fact that irradiation enhances the diffusion process. As far as the present situation is concerned, this fact cannot be ignored. The reason is that the displacement rate of atoms under ion irradiation can in this case reach $\sim 10^{-4}-10^{-1}$ displacements per atom per second (as compared to $\sim 10^{-7}-10^{-5}$ or fewer displacements per second for nuclear reactor materials after one-year exposure to neutron irradiation [14]). For these reasons, there is a wide range of materials, including refractory ones, where effective diffusion and the effective removal of atoms from the neutron irradiated zone can be observed for exposure times of tens of seconds to thousands of minutes at relatively low temperatures, for example, at room temperature. The selectively removed atoms reaching that outer surface of the material facing the beam (vacuum) can, if they are gaseous atoms, evaporate into the vacuum and escape irreversibly from the material. As a result, the selectively removed atoms displaced to interstitial positions develop a concentration gradient in the direction of the surface facing the beam. Because the outer surface is a nonsaturable sink, the removed atoms continue to evaporate from this surface until they arrive at it via diffusion through interstitial positions, i.e., until all the atoms are removed from the material. Clearly, the higher the temperature, the faster the removed atoms diffuse. We note that as the temperature increases, the SRA rate and the rate of chemical composition change increase until the rate of the radiation-induced displacement of selectively removed atoms becomes a limiting factor for SRA processes.

In principle, any boundary (not only the outer one) can serve as a sink for knocked-out atoms. For example, in Ref. [15], a boundary between a silicon single crystal and a 50 nm thick layer of thermal oxide was a sink for defects that proton radiation created in silicon. The accumulation of defects in a thin ($\sim$ 3 nm) silicon layer bordering the oxide resulted in its becoming amorphous, whereas in the remainder of the sample, where most of the defects were produced, the concentration of defects did not reach the critical value, and the material remained largely crystalline, except for vacancy and interstitial clusters that concentrated most at the depth $\sim$ 40 nm from the interface. In relation to the problem discussed here, of much importance are the capabilities of the above-listed boundary types as sinks for SRA.

The data we obtained on the effect of temperature on the SRA rate are direct experimental evidence of the role of diffusion processes in SRA. This effect is estimated by measuring the dose dependences of the electrophysical and/or magnetic properties that are involved in insulator–metal or nonmagnetic–magnetic transitions and are due to changes in the chemical composition of the irradiated material (Fig. 8). The data in Fig. 8 on the dose dependence of the electric resistance of cobalt oxide at various irradiation temperatures show that for a fixed ion flux density, increasing the irradiation temperature can lead to a multiple increase in the SRA rate. That diffusion processes are of crucial

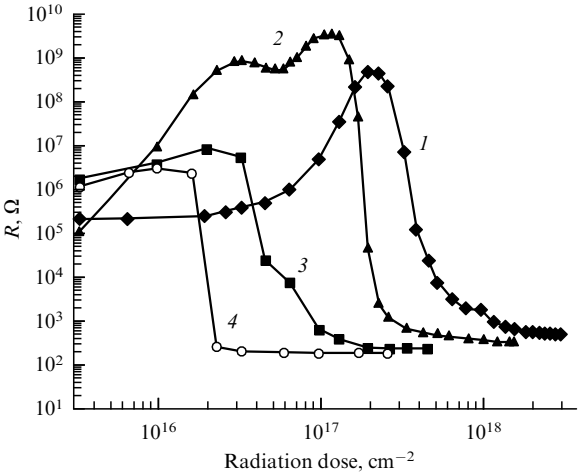

Figure 8. Dose dependence of the reduction in Co_3O_4 40 nm thick for the proton energy 3 keV at the radiation temperature 50 °C (*1*), 100 °C (*2*), 150 °C (*3*), and 200 °C (*4*).

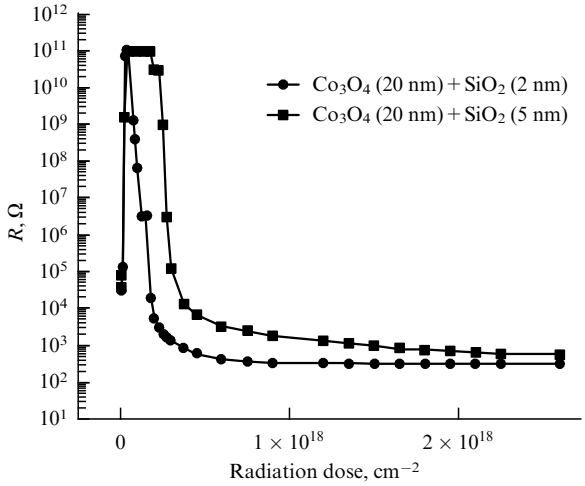

Figure 9. Dose dependence of the reduction of Co_3O_4 20 nm thick irradiated by 1.2 keV protons through a silicon oxide layer of thicknesses 2 and 5 nm.

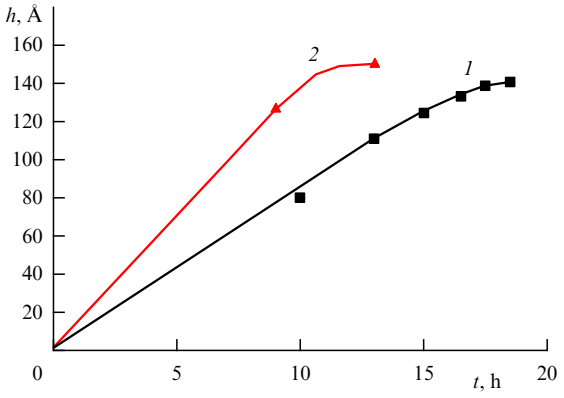

Figure 10. The thickness of oxide-reduced cobalt as a function of the duration of proton irradiation at 1.6 keV at 9.12 mkA cm^{-2} (*1*) and 13.68 mkA cm^{-2} (*2*).

importance for SRA is seen from the experimental data that demonstrate radical changes in the composition and properties of chemical compounds that have been irradiated through intermediate layers of other monatomic or more complex materials (Fig. 9). Importantly, this does not necessarily change the composition of the intermediate layers. Thus, irradiation through monatomic (for example, tungsten) or diatomic (for example, silicon oxide) intermediate layers does not change the chemical composition of the layers but results in hydrogen atoms being selectively removed from the lower lying layers of cobalt oxides (and other materials).

We consider how diffusion processes lead to the irreversible removal of knocked-out atoms from the irradiation zone and affect chemical composition during the SRA process. To implement a diffusion process, it is necessary that there be a diffusant and that the diffusant concentration have a gradient. This follows directly from the classical diffusion equations

$$J = -D\frac{\partial C}{\partial x}\,, \tag{5}$$

$$\frac{\partial C}{\partial t} = D\frac{\partial^2 C}{\partial x^2}\,, \tag{6}$$

where J is the diffusant flux density, D the diffusion coefficient, and C the diffusant concentration.

For chemical compounds that are stable at the irradiation temperatures studied, diffusant atoms are those being selectively removed (usually, the constituent species whose displacement rate is maximum). Their appearance in noticeable concentration in the irradiation zone is a radiation-induced effect, which, in accordance with Eqns (5) and (6), determines the diffusional outflow of knocked-out atoms from the irradiation zone to sinks or to the nonirradiated regions of the material. For the same reason, the SRA rate (with all the other factors unchanged) is proportional to the ion flux density in the beams used. Figure 10 shows that increasing the beam current density by a factor of 1.5 produces an increase by the same factor of 1.5 in the saturation time of the thickness of reduced cobalt.

Thus, in the stability temperature range of the chemical compounds chosen, the only source of diffusant is the radiation-induced displacements of the corresponding atoms in the course of irradiation.

In considering possible directions for diffusant concentration gradients in an irradiated material, two very different situations can be distinguished. The first occurs when the unmasked material is irradiated by a uniform (in intensity) flux of ions; in the second, the irradiated material is covered by a mask consisting of an array of holes whose size is less than or comparable to the projected range of the accelerated particles in the material.

In the mask-free case, the only possible direction for the radiation-induced diffusant concentration gradient is perpendicular to the surface of the sample. We note that in this case, in the temperature range of thermal stability of the chemical compounds being treated, the atoms to be removed do not take part in forming the concentration gradient if they reside in lattice sites belonging to their species subsystem or occupy stable positions corresponding to short-range order configurations characteristic of amorphous materials. For this reason, the only atoms that are to be removed and that form a concentration gradient are those that occupy interstitial positions or vacancies belonging to a different atomic subsystem (because these positions are less stable than the original ones). Diffusion causes such atoms to leave the irradiated volume toward either the outer (vacuum-facing) boundary or the interior of the material. In the former case, the displaced atoms evaporate into the vacuum if they are gaseous or can form gaseous compounds with residual gases there (or with accelerated beam atoms or ions). This, combined with irradiation, allows retaining the concentration gradient and maintaining SRA. This fact sets selectively removed atoms fundamentally apart from other compound-forming atoms that cannot evaporate from a surface and for which there are therefore no easy and effective ways of removal from the surface and hence of retaining the concentration gradient. Precisely because of this, a difference in displacement rates between constituent atoms is unimportant if diffusion processes play an important role. The efficient combination of diffusion with subsequent removal of targeted atoms from the surface allows the SRA rate to increase with an increase in the energy of beam ions. Herein lies a fundamental difference between SRA and the redistribution of components in several near-surface layers (with a thickness ~ 1 nm) using physical sputtering. In the latter case, increasing the energy

of the particles makes changes in the component ratio inconsequential.

When the removed atoms diffuse toward the interior of the sample, conditions for keeping their concentration gradient sufficiently high in this direction are much worse. Still, it proved possible to experimentally detect the presence of removed atoms in lower-lying layers.

In this experiment, proton radiation was directed on a thin film sandwich, with the top (beam-facing) layer made of the oxide of a nonmagnetic metal and the bottom layer made of pure metallic magnetic cobalt. The fact that part of the oxygen atoms removed from the top layer moved toward the bottom layer was detected by a decrease in the saturation magnetization of the samples due to the formation of nonmagnetic cobalt oxide as a result of oxygen atoms entering the bottom layer. As seen from Fig. 11, the contribution from this effect was about 10%, much more than the possible measurement error. We note that for pure cobalt, irradiation under similar conditions, with no layers added on top, does not decrease the saturation magnetization up to large fluence values until a marked sputtering of the sample is observed. These experiments showed that under the irradiation conditions used, only a minor part of selectively removed atoms diffuse along the direction of the beam.

If irradiation is through a mask with a regular array of holes whose size is less than or comparable to the projected range of the accelerated particles in the material, additional outflow directions become available for selectively removed atoms. This is because selectively removed atoms may then also have a concentration gradient perpendicular to the surfaces that are formed by the holes of the mask and which separate the irradiated regions from nonirradiated ones. The displaced atoms that enter the nonirradiated regions can then diffuse toward the outer, beam-facing surface and leave the material there much in the way discussed above for the no-mask case. The additional SRA sinks available when using a mask accelerate the removal processes from the irradiated regions of the material. With all the other factors unchanged, this acceleration becomes larger as the holes become smaller. Clearly, a practically similar situation must occur when creating high-density patterned nanostructures, i.e., structures with the element sizes and separations less than ~ 100 nm.

Direct experiments show that for selectively removed atoms to leave a layer of a chemical compound irradiated through a layer of an intermediate material, it is not fundamentally necessary that the material of the upper intermediate layer contain vacancies. In these experiments, a layer of nonmagnetic cobalt oxide was irradiated through a tungsten layer 5 nm thick. The proton energy was only 300 eV, by far not enough to displace tungsten atoms, whose threshold displacement energy is 42–44 eV [16]. However, as evidenced by an increase in the saturation magnetization compared to the nonirradiated values (Fig. 12), oxygen atoms were selectively removed from cobalt oxide. The original samples exhibit magnetic properties because of a partial reduction in cobalt oxide due to the layer of tungsten deposited on the top surface. Because selectively removed atoms can leave the irradiation zone by diffusing via interstitial positions (at temperatures where the corresponding chemical compounds are thermally stable), it turns out that the influence of temperature on the SRA rate may be considerable for many materials even at relatively low temperatures (for example, room temperature). Experiments on the effect of temperature on the SRA rate reveal that increasing the temperature not only leads to a considerable acceleration of SRA (see Fig. 8), which is no surprise for diffusion-related processes, but also markedly decreases the number of displacements per atom required for them to be practically completely removed. For example, in proton-irradiation oxygen-removal experiments on cobalt oxide at various temperatures, the degree of removal was estimated from how consistent the magnetic properties of irradiated films were with their tabulated values. It was found that increasing the irradiation temperature from 80 °C to 200 °C decreases the number of displacements per atom by ~ 3 to 3.5 times, which means that virtually all nonmagnetic cobalt oxide became magnetic metallic cobalt (Fig. 13).

One possible factor affecting the dose level required to achieve the complete reduction is the diffusion length for oxygen atoms knocked out from their regular lattice positions. The term diffusion length refers to the average distance over which a knocked-out atom diffuses before annihilating with a vacancy in its own subsystem. Because the diffusion length increases with the temperature (that is, for intermediate temperatures for which the mobility of interstitial atoms

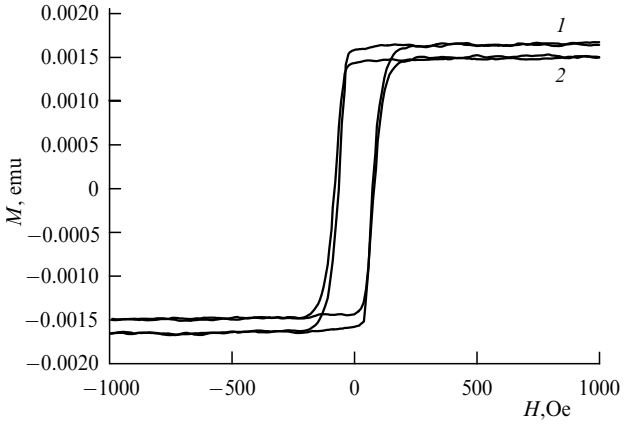

Figure 11. Change in the magnetization curve of 20 nm thick cobalt film irradiated by 1.5 keV protons through a 75 nm copper oxide layer: (*1*) before irradiation; (*2*) after irradiation.

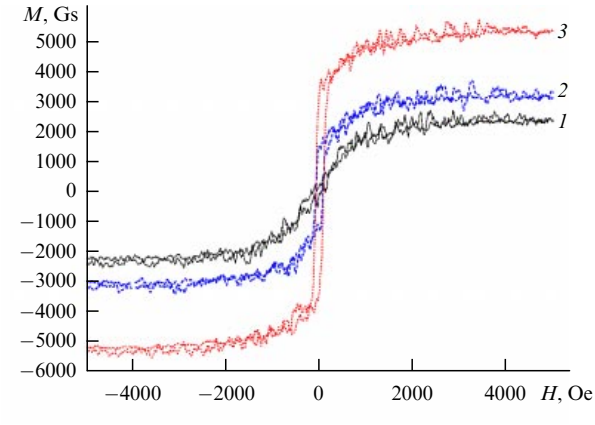

Figure 12. Change in the magnetization curve of a 40 nm thick cobalt film irradiated by 0.3 keV protons through a 5 nm tungsten layer: before irradiation (*1*); after irradiation at 2×10^{18} cm^{-2} (*2*) and 4×10^{18} cm^{-2} (*3*).

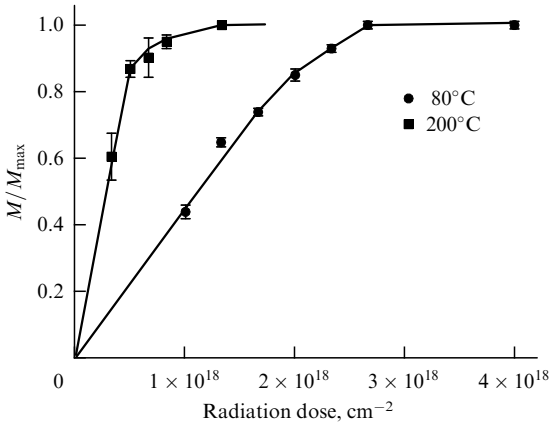

Figure 13. Change in the magnetic properties of Co_3O_4 oxide 80 nm in thickness irradiated with protons with the energy 3 keV as a function of the dose at different irradiation temperatures.

increases faster than that of vacancies because of a considerable difference in the diffusion activation energy between defects of these types), it is clear that after a single knocking-out event, a knocked-out atom diffuses, on average, farther in the direction toward the sink, in accordance with the concentration gradient. For an oxygen atom to move further, a new knocking-out event is required. The larger the diffusion length, the fewer such events are needed for the oxygen atom to reach the corresponding sink, where it leaves the system forever. In spite of the above, the change in the diffusion length with increasing the temperature is unlikely to explain the qualitative differences observed in the temperature dependences of the radiation damageability of a wide class of materials. The reason is that, on the one hand, the diffusion length changes with increasing the temperature in a similar qualitative way for practically all materials, but on the other hand, increasing the temperature decreases the radiation damageability of monatomic materials and solid solutions but decreases that of chemical compounds.

Along with the fact that the diffusion rate increases with increasing the temperature, another possible reason for this decrease is that the threshold displacement energy of oxygen decreases with increasing the irradiation temperature. The increase in the threshold energy with temperature was observed by the present authors in graphite [17, 18] and is also known to occur in a number of other materials, including atoms that comprise oxides [19]. Another reason why the number of displacements per atom decreases down to a complete transformation of the material may be the fact (documented, e.g., in Refs [20, 21]) that the radiation damage of chemical compounds becomes much less reversible as the irradiation temperature increases. This seems to be of particular relevance to chemical compounds with a relatively low chemical affinity (binding energy) between their constituent atoms. Clearly, radiation damage should be particularly irreversible for chemical compounds consisting of atoms with low binding energy (and hence with a low threshold displacement energy). An extreme example is provided by gaseous atoms, for which no spatial configurations (including those after radiation damage) can conceivably repeat themselves in time.

It is well known that for monatomic crystals (we do not consider di- or polyatomic compounds here), increasing the irradiation temperature decreases the efficiency of radiation damageability (i.e., decreases the number of displacements per atom required on average to produce a single surviving defect). That is, at a higher irradiation temperature, more displacements per atom are needed for the same number of defects to survive. For monatomic materials, this immediately implies that as the irradiation temperature increases, a higher dose (fluence) of irradiation is needed to achieve the same change in lattice parameters (physically, because of the increased recombination efficiency of point defects and the arrival of points defects at sinks).

As mentioned above, the situation is different for diatomic compounds. In this case, the SRA process involves a phase transition and the corresponding transformation of the crystal lattice of the chemical compound into that of a monatomic material, with a marked ($\sim 50\%$) reduction in the volume of the material [5], all this resulting from effective radiation damage, i.e., from those point defects that were not ultimately involved in the annihilation event. A very significant fact that we discovered (and which was already mentioned above) is that the efficiency of radiation damage increases with the irradiation temperature. Because in all materials, both monatomic ones and chemical compounds, point defects become more mobile with increasing the irradiation temperature, it can be hypothesized that the fundamental difference between monatomic materials and chemical compounds in how the efficiency of radiation damageability varies with the irradiation temperature is rooted in the fact that chemical compounds have a lower probability of annihilation between displaced atoms and their corresponding vacancies (i.e., vacancies belonging to the corresponding system of atoms, for example, of oxygen atoms in oxides). Ultimately, then, it is most likely that with all other radiation conditions being equal, the efficiency of radiation damageability and SRA in chemical compounds greatly depends on the chemical affinity of their constituent atoms.

The irreversible movement of displaced atoms of a given species toward the surface facing the beam of accelerated particles can be strongly affected by ascending diffusion, due to internal interlayer stresses that inevitably develop in the process of irradiation as a result of considerable volume changes in the irradiation zone. This mechanism allows the removed atoms to diffuse in all directions from the irradiation zone; however, in the absence of heating, only its vacuum-bordering outer surface is a nonsaturated sink: when reaching this surface, selectively removed atoms (for example, atoms of oxygen, nitrogen, or hydrogen) evaporate into the vacuum and leave the material. Additional special studies are needed to quantify the influence of ascending diffusion on SRA processes.

When a masked-radiation SRA technique is used to fabricate patterned nanostructures, two factors are to be taken into account: shrinkage-related stresses (see above) and stresses at the lateral surfaces of the irradiated regions (elements), that is, the boundaries of the mask holes. These stresses also stimulate the ascending diffusion of removed atoms in the direction normal to these surfaces. If mask holes are sufficiently small in size (for example, a few tens of nanometers), this mechanism can lead to a markedly faster removal of atoms from the irradiation zone.

6. The role of the chemical factor in SRA

There are two aspects pertaining to the chemical factor as related to the SRA process under irradiation. The first is chemical interaction between the accelerated beam particles

and the chemical compound being irradiated. In relation to the results available and conditions investigated, the following point should be made.

The selective removal of atoms at irradiation temperatures close to or somewhat above room temperature is observed to occur for irradiation by electrons, protons, and helium atoms, which conclusively indicates that the chemical nature of the accelerated particles is not in itself of fundamental significance. Besides, as evidenced by step-by-step XPS studies of chemical composition (Fig. 14a), in the temperature range studied (from about 20 °C to 250 °C), SRA practically starts directly from the upper layer of the chemical compound that faces the beam of accelerated particles. For typical proton energies ($\sim 1-5$ keV), the zone of most radiation damage has a different position along the thickness of the chemical compound than the zone where most of the hydrogen atoms from the incident beam stop in their motion. Based on SRIM calculations [8], the zone where most beam atoms stop (the ions are neutralized when penetrating the material) is considerably below (usually, by tens of nanometers) the zone of most intense radiation damage (Fig. 14b). If a purely chemical mechanism dominates, then on the distribution profiles of light elements in films of chemical compounds, the atoms of the second remaining component would be expected to primarily concentrate toward the surface of the compound layer, where the beam leaves the material. This kind of effect, however, has never been observed in the irradiation temperature range studied, although it is possible in principle that purely chemical mechanisms play a more significant role at higher temperatures.

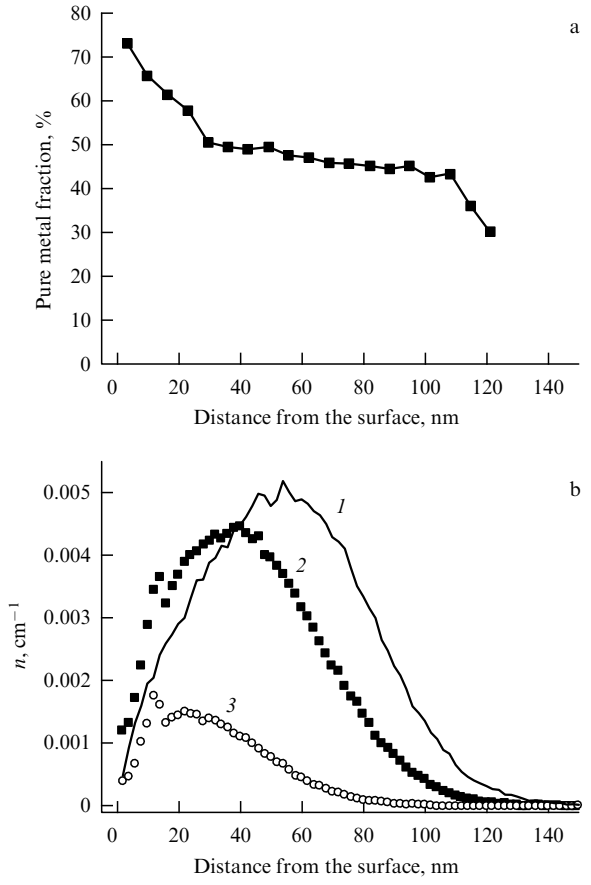

Figure 14. (a) Through-thickness profile of tantalum reduction in a 120 nm thick tantalum oxide film irradiated with 5 keV protons. (b) Calculated distribution profiles of implanted hydrogen atoms (*1*), vacancies for oxygen atoms (*2*), and tantalum atoms (*3*).

The second aspect pertaining to the chemical factor in selectively removing atoms from chemical compounds is the chemical affinity of the constituent atoms. As a knocked-out atom moves in the volume of the compound toward its corresponding sink, it interacts with other atoms of the lattice and thus forms links with its closest lattice environment. Early in the irradiation, these links may fully correspond to or differ from the original (prior to knocking out) links; the former situation occurs if a migrating atom recombines with a vacancy on the same subsystem of atoms, and the latter if the current position is interstitial or if the atom encounters a vacancy belonging to a different subsystem. As the concentration of selectively removed atoms decreases, the links change in nature and strength due to the rearrangement of the atomic structure of the matrix (for example, stoichiometric changes of the matrix or phase transformations due to irradiation).

Clearly, the more weakly the selectively removed atoms are linked to their original environment in the chemical compound, the less likely they are to annihilate with vacancies. It is also expected that these compounds have a lower energy threshold for SRA. In general, with all irradiation conditions being equal, chemical compounds consisting of atoms with a weak chemical affinity are expected to require smaller radiation doses to free themselves from selectively removed atoms. Calculating the exact values of the characteristic binding energies of atoms in chemical compounds is a challenging task. In our view, the chemical affinity of atoms in diatomic compounds and their associated binding energies might be qualitatively estimated based on the hydrogen potentials of the chemical activity of the element constituting the basis of the matrix being modified. In other words, the smaller the potential, the more active is the element. It is logical to assume that lower values of the potential correspond to higher-energy local links of a knocked-out atom in the matrix, correspondingly making it more difficult to remove atoms from such a matrix. For compounds with a relatively higher chemical affinity, i.e., with a lower potential of removed atoms, knocked-out atoms are likelier to recombine with the vacancies of their own subsystem, increasing the dose needed for the complete removal of the chosen atomic species. Table 3 summarizes the values of the hydrogen potential for various elements.

The vast body of experimental data available on the selective removal of oxygen atoms from various oxides generally supports the arguments above. With all other radiation conditions being equal, and assuming a similar extent of removal, the time needed to remove oxygen from the film of an oxide of an element increases in the following succession: Pt, Pd, Ag, Co, Cu, Re, Bi, W, Pb, Sn, Ge, Mo, Ni, Fe, Ga; the oxides of the next two elements, As and Cr, do not reduce; then follow oxides of Ta and Ti; the oxide of Si does not reduce; then follow oxides of Nb and V; the oxide of Al does not reduce (the oxides of the skipped elements were not studied; see Table 3). At the same time, the results presented and, first and foremost, the failure to remove oxygen atoms from oxides of intermediate-activity elements indicate the multifactor nature of the phenomenon under study.

One possible reason for the discovered exceptions is that the chemical activity data in Table 3 were obtained under

Table 3. The hydrogen activity series for elements.

Element	Hydrogen potential	Element	Hydrogen potential
La	−2.5	Mo	−0.2
Sc	−2.1	Ge	−0.15
Al	−1.66	Sn	−0.14
V	−1.2	Pb	−0.13
Nb	−1.1	W	−0.09
Si	−0.86	H	0
Ti	−0.86	Bi	0.21
Ta	−0.8	Re	0.3
Zn	−0.76	Cu	0.33
Cr	−0.74	Co	0.33
As	−0.68	Ag	0.8
Ga	−0.56	Pb	0.987
Fe	−0.44	Pt	1.2
Cd	−0.4	Au	1.5
Ni	−0.23		

markedly different conditions from (and hence do not apply to) the experiments we consider here. Another reason might be that measures to compensate the additional charge when sending a beam of ions on a quality dielectric were not taken, with the result that the radiation process rapidly loses efficiency due to the effect of sample charges.

There is finally one more note. It is clear from the discussion above that in the absence of external sources from which atoms of the species being removed could be entered into the irradiated layer of chemical material, the selective removal of these atoms from the layer (for example, due to evaporation into the vacuum in the case of oxygen) becomes inevitable. However, the situation can be quite different if some external source(s) does (do) supply atoms of the same type as those being removed. With all other conditions being the same, the external source for compensating the operation of the SRA mechanism should be less intense for a higher chemical affinity of the constituent atoms of the chemical material being irradiated. In real experiments, external sources for supplying atoms of some species to irradiated layers can be due to the presence of residual gases (e.g., oxygen) in vacuum facilities. In this case, clearly, the effect of such a source can be blocked, if only temporarily, by separating the irradiated layer from direct contact with the vacuum by a layer of an intermediate auxiliary material, whose thickness is much less than the range of the accelerated particles used. How effectively this can be done may depend on the properties of the auxiliary layer, including its thickness, chemical properties, and the diffusion coefficient for the corresponding atomic species. Our direct experiments showed that auxiliary layers allow considerable SRA effects to be obtained in chemical compounds for which it is otherwise impossible. Figure 15 shows the results of a layer-by-layer analysis of a silicon oxide sample irradiated through auxiliary layers of metals with different chemical affinities. It is seen that the higher the activity of the auxiliary layer, the greater the reduction in silicon from the oxide. We emphasize that the reduction in

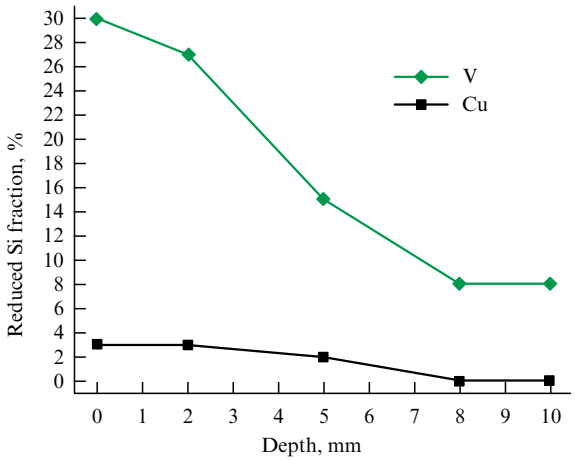

Figure 15. Through-thickness profile of oxide-reduced silicon after 1500 eV proton irradiation through 10 nm thick auxiliary layers of copper and vanadium.

silicon from irradiated oxide has never been observed in experiments without an auxiliary layer.

Another series of direct experiments confirmed the earlier suggestion that it is oxygen coming from the vacuum that prevents the SRA of oxygen when compounds such as oxides of silicon and aluminum are irradiated by protons. In these experiments, in which pure silicon and aluminum were irradiated by protons under standard conditions, the formation of the corresponding oxides down to depths of more than 10 – 20 nm was demonstrated using XPS. This means that even the relatively high oilless vacuum typical of our irradiation experiments is no guarantee that oxygen (most likely, in the form of accelerated ions) does not enter the samples.

7. Estimating the spatial delocalization of the zone of chemical composition change

From the standpoint of using the effect and technique of SRA to create functional nanostructures and nanoelements for various uses, it seems important to understand if and how it is possible to maximally reduce the size of the zone where the properties and chemical composition of the material are controllably changed. We consider the factors potentially delocalizing the irradiation zone and hence the zone where the chemical composition is being changed (meaning that the zone of changing composition in the material being treated moves beyond the irradiation zone whose boundary is determined by the mask holes). Of key importance in this context is the scale factor, comprising the size of the irradiated region and the thickness of the material in which the chemical composition is to be changed. The region where chemical composition is to be transformed is extremely small in size, $\sim 1 - 10$ nm. A suitable situation occurs when a material $\sim 3 -$ 30 nm thick is irradiated with accelerated particles (for example, protons) of the above-mentioned energies through a resist mask with appropriate size holes spaced ~ 100 nm apart.

We consider this situation in relation to an experiment in which a 10 nm thin film, for example, of cobalt oxide on a substrate of monocrystalline silicon is irradiated by a beam of 0.5 – 3.0 keV protons. In this case, for a beam with small angular divergence and for medium atomic number materials, the average projected range of a proton is about 100 nm. If the thickness of the oxide layer is approximately equal to the

mean free path of the incident protons, then a passing proton undergoes only a single interaction with a target atom within this layer, i.e., there is only one event in which an oxygen atom is knocked out of a crystal site. All secondary knockouts occur at larger depths beyond the working layer. It is primarily the possibility of a transformation occurring in the region of the first displacing collision of a proton with an oxygen atom in the working layer that allows the use of SRA for creating extremely small-size nanoscale elements, including those of high density.

Thus, as far as the above reason is concerned, the way to prevent the delocalization of the zone of controllable composition change is by not using excessive proton fluences.

Another possible cause of delocalization is energy exchange between selectively removed atoms and neighboring atoms following the formation of a PKA due to a collision with a proton. Because the energy of a PKA cannot exceed ~ 200 eV in this case and because the free path of a PKA is in fact one atomic spacing, it follows that the delocalization due to this process is ~ 1 nm.

One further possibility is the backscattering of protons from regions beyond the irradiation region, followed by the displacement of removed atoms in this region. It is easy to show that the probability of this process is proportional to the volume of the irradiated region and inversely proportional to the distance between irradiated regions. This means that if excessive proton fluences are not used when using radiation to controllably change the chemical composition (not even after the complete removal of the atoms of the targeted species), then the delocalization of the irradiation zone that is related to backscattering is negligible. This implies that, given the correct choice of parameters, using accelerated ions (atoms) in principle allows achieving sizes $\sim 2-3$ nm and densities about 10,000 Gbit inch^{-2} for regions of controllable composition change (in multilayered structures in particular). If the maximum energy transfer from accelerated particles to removed atoms exceeds the threshold displacement energy of the latter only slightly, then the controlled change regions can in principle be even less in size and higher in density because of the practically total absence of delocalization.

We estimate how far an ion can deviate radially over its mean free path before its first displacing interaction with a target atom occurs. If the mean free path for interaction with the ion subsystem is L, then the deviation of an ion from the rectilinear trajectory is determined by all scattering interactions it undergoes with the electron subsystem over a trajectory segment of the length L. Because each scattering event transfers only a small amount of energy to electrons (electrons have a small mass!), the energy of an ion can be considered constant until the first scattering on the atomic subsystem.

We let l_e denote the mean free path of an ion between two interactions with electrons. Then, with α_e denoting the maximum scattering angle of the ions, a conservative estimate of the maximum deviation angle of the ion from the rectilinear trajectory is given by

$$\alpha_{max} = \alpha_e \frac{L}{l_e} . \tag{7}$$

The maximum deviation the ion acquires in the plane perpendicular to the line of incidence is

$$R_{max} = L \tan \alpha_{max} = \alpha_e \frac{L^2}{l_e} . \tag{8}$$

Because $L = 1/(\sigma_d n_a)$ and $l_e = 1/(\sigma_e n_e)$, where σ_d is the cross section for the displacing scattering of an ion on the atomic subsystem, σ_e is the cross section on the electron subsystem, and n_a and n_e are the atom and electron number densities, we can also write

$$R_{max} = \frac{\alpha_e \sigma_e n_e}{(\sigma_d n_a)^2} . \tag{9}$$

An estimate of the maximum scattering angle of an ion in the process of interaction with an electron can be obtained from the relation

$$\sin \alpha_e \cong \alpha_e = \frac{m_e}{m_i} , \tag{10}$$

where m_e and m_i are the masses of the electron and the ion. For cobalt oxide Co_3O_4 irradiated by 1 keV protons, the maximum deviation from the rectilinear trajectory is estimated to be

$$R_{max} = \frac{m_e}{m_i} \frac{\sigma_e n_e}{(\sigma_d n_a)^2} \approx \frac{1}{1836} \ 9000 \text{ Å} \approx 5 \text{ Å} . \tag{11}$$

This means that, conservatively, the axial deviation of an ion from the rectilinear trajectory before the first displacing collision is a few fractions of a nanometer, implying that with the above thickness and dose constraints, it is in principle possible to create superdensity structures with the use of SRA. In the general case, the calculation of the minimum achievable distance between the elements of a structure requires calculating the defect-generation density over the volume of the substrate, taking into account factors such as the topology of holes in the mask, the working layer and substrate materials, the energy of the particles, and the dependence of the service performance of the material on the dose level.

The maximum density currently achievable with ion irradiation and SRA for regions we consider here (those where the chemical composition and other properties are being locally modified) depends on the possibility of creating high-density patterns of holes in resist masks by using electron lithography or nanoimprint lithography techniques. The best result to date, 153 Gbit inch^{-2} (see Fig. 16), was achieved in an SRA experiment in which a two-dimensional periodic pattern of vertical cobalt magnetic bits was created in a cobalt oxide film 80 nm thick, the bits being 15 nm in diameter and 30 nm in height and spaced 50 nm apart.

8. Conclusion

Recent studies by the present authors and colleagues (see Refs [6, 9, 10, 22–24]) have demonstrated the great methodological and technological promise the SRA effect has as a tool for the direct parallel design of functional structures and nanoelements for various applications. The experiments performed revealed the complex physical nature of the SRA effect. Although the atoms to be removed are displaced in a purely mechanical way in the process of the interaction of accelerated particles with the irradiated material, what happens to them afterwards is determined by a variety of processes. Because these processes are different from the physical (collisional) sputtering of atoms, it proves possible not only to extend SRA to a large depth (100 nm or more) but also to penetrate it through intermediate layers of

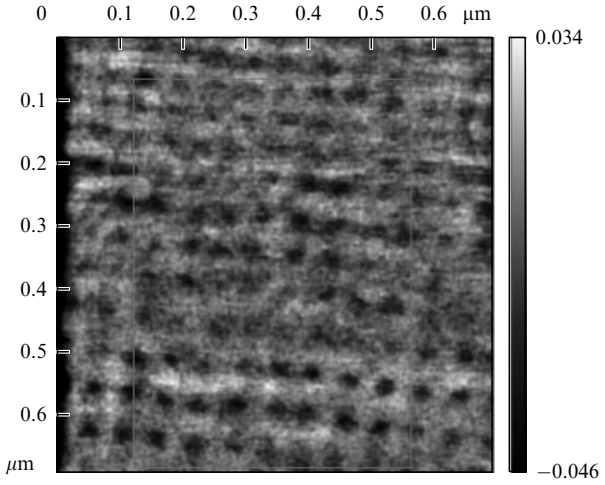

Figure 16. Magnetic image of an SRA-fabricated patterned medium with vertically anisotropic cobalt bits. The bits are 15 nm in diameter, 30 nm in height and 50 nm spaced).

other materials. In most cases, the selective removal of atoms after their displacement is by diffusion toward sinks, with the result that the change rates of the composition and properties of the irradiated materials are strongly dependent on temperature. With all the above features, irradiation through a mask allows carrying out parallel (simultaneous) composition and property transformations in various layers of multilayered thin film materials, such that the self-compatibility of different elements of the newly created structures is ensured in different layers.

The experiments we report reveal that there is a fundamental difference in the temperature dependence of radiation damageability between monatomic materials (including solid solutions) on the one hand and chemical compounds on the other. It is found that the efficiency of the radiation damageability of (and the rate of the selective removal of atoms from) chemical compounds are larger, the smaller is the chemical affinity of their constituent atoms. This is presumably because an increase in the chemical affinity of atoms comprising a chemical compound, with all other factors being equal, decreases the probability of the selectively removed atoms annihilating with vacancies in their own atomic subsystem.

Both theoretical estimates and experimental data show that SRA holds vast promise for creating superdensity functional nanostructures for various uses. However, further studies of the physical aspects of SRA are needed for this method to be effectively applied in practice. Having in mind new experimental possibilities expected to be available in the near future, the authors propose conducting experimental measurements of the threshold displacement energies of atoms in various chemical compounds at various temperatures. This should help to elucidate the relation between the threshold displacement energy and the chemical affinity of atoms in chemical compounds, thus allowing numerical simulation methods to be developed to model observed effects. It is also necessary to conduct direct experiments to quantitatively investigate the delocalization of the SRA zone in relation to the mask-defined geometrical boundary as a function of irradiation conditions (the ion energy and the dose and temperature of irradiation). Such experiments would provide limit values that can be achieved with SRA for the resolution of the method and for the density of patterned structures.

Acknowledgements. We are deeply grateful to our colleagues for their assistance in carrying out the work and conducting some experiments, and also for their helpful discussions: D I Dolgii, A G Domantovskii, E A Kuleshova, K I Maslakov, E D Ol'shanskii, and V L Stolyarov. This work was supported by the Russian Federal Agency for Science and Innovation.

References

1. Gurovich B A et al. *Usp. Fiz. Nauk* **171** 105 (2001) [*Phys. Usp.* **44** 95 (2001)]
2. Gurovich B A et al. *Microelectron. Eng.* **69** 358 (2003)
3. Gurovich B A, Domantovskii A G, Maslakov K I, Prikhod'ko K E *Poverkhnost'. Rentgen., Sinkhrotron. Neitron. Issled.* (10) 67 (2004)
4. Gurovich B A et al., in *Nanostructured Magnetic Materials and Their Applications* (Eds B Aktas, L Tagirov, F Mikailov) (Dordrecht: Kluwer Acad. Publ., 2004) p. 13
5. Gurovich B A, Domantovskii A G, Maslakov K I, Prikhod'ko K E *Poverkhnost'. Rentgen., Sinkhrotron. Neitron. Issled.* (5) 25 (2008) [*J. Surf. Invest. X-Ray, Synchr. Neutron Tech.* **2** 352 (2008)]
6. Gurovich B et al. *Proc. SPIE* **6260** 626005 (2006)
7. Prikhod'ko K E *Voprosy Atom. Nauki Tekh. Ser. Fiz. Radiats. Povrezhdenii Radiats. Mater.* (3) 36 (2002)
8. Ziegler J F, Biersack J P, Ziegler M D *The Stopping and Range of Ions in Matter* (Morrisville, NC: Lulu Press Co., 2008); http://www.srim.org
9. Gurovich B A et al. *Fiz. Tekhn. Poluprovodn.* **38** 1074 (2004) [*Semiconductors* **38** 1036 (2004)]
10. Domantovskii A G, Gurovich B A, Maslakov K I *Crystallogr. Rep.* **51** (Suppl. 1) S196 (2006)
11. *International Technology RoadMap for Semiconductors. Process Integration, Devices and Structures* (2007) p. 6; http://www.itrs.net/Links/2007ITRS/2007_Chapters/2007_PIDS.pdf
12. Kelly B T *Irradiation Damage to Solids* (Oxford: Pergamon Press, 1966) [Translated into Russian (Moscow: Atomizdat, 1970)]
13. Dzhafarov T D *Radiatsionno-stimulirovannaya Diffuziya v Poluprovodnikakh* (Radiation-Stimulated Diffusion in Semiconductors) (Moscow: Energoatomizdat, 1991)
14. Akasaka N et al., in *Effects of Radiation on Materials*: *21st Symp.* (ASTM Special Technical Publ., Vol. 1447, Eds M L Grossbeck et al.) (West Conshohocken, PA: ASTM Intern., 2004) p. 516
15. Smirnov L S *Fizicheskie Protsessy v Obluchennykh Poluprovodnikakh* (Processes in Irradiated Semiconductors) (Novosibirsk: Nauka, 1977)
16. Maury F et al. *Radiat. Effects Defects Solids* **38** 53 (1978)
17. Gurovich B A Prikhodko K E *Radiat. Effects Defects Solids* **154** 39 (2001)
18. Prikhod'ko K E, Gurovich B A *Voprosy Atom. Nauki Tekh. Ser. Fiz. Radiats. Povrezhdenii Yavlenii Tved. Telakh* (4) 34 (2000)
19. Hren J J, Goldstein J I, Joy D C (Eds) *Introduction to Analytical Electron Microscopy* (New York: Plenum Press, 1979) [Translated into Russian (Moscow: Metallurgiya, 1990)]
20. Barnard R S, Ph.D. Thesis (Cleveland, OH: Case Western Reserve Univ., 1977)
21. Pells G P, Phillips D C, UKAEA Res. Rep. AERE-R9138 (1978)
22. Gurovich B et al., in *Magnetic Nanostructures* (Springer Ser. in Materials Science, Vol. 94, Eds B Aktas, L Tagirov, F Mikailov) (Berlin: Springer, 2007) p. 47
23. Gurovich B A et al. *Nano- Mikrosistem. Tekh.* (4) 2 (2007)
24. Gurovich B A et al. *Prikladnaya Fiz.* (1) 44 (2008)